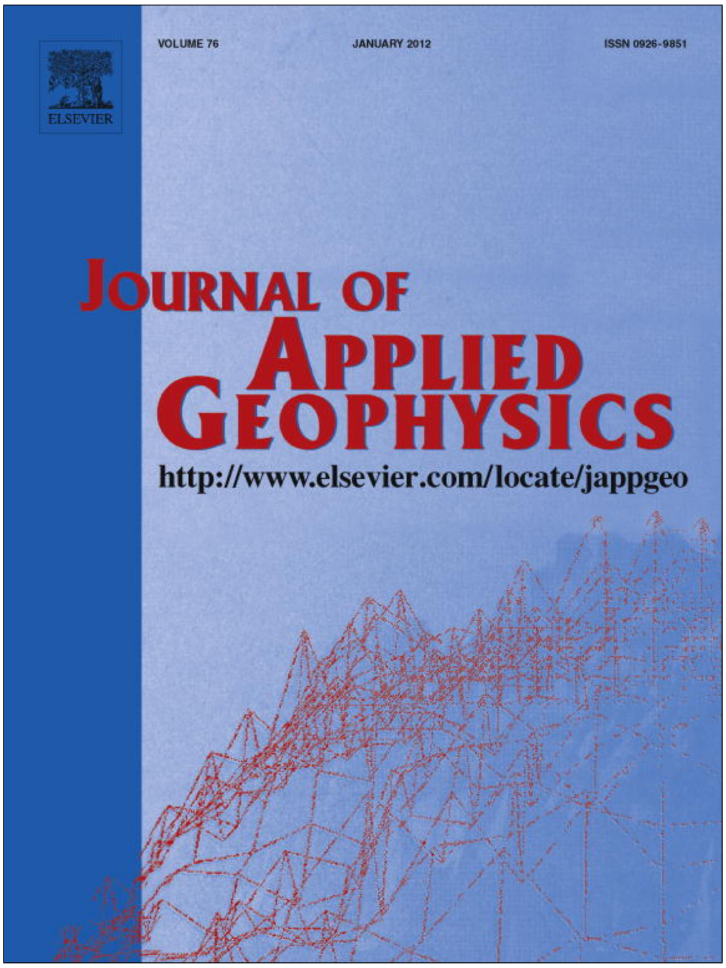
VOLUME 76
JANUARY 2012
ISSN 0926-9851
ELSEVIER
JOURNAL OF APPLIED GEOPHYSICS
http://www.elsevier.com/locate/jappgeo

Journal of Applied Geophysics 80 (2012) 121–128

Contents lists available at SciVerse ScienceDirect

Journal of Applied Geophysics

journal homepage: www.elsevier.com/locate/jappgeo

Seismic results as a-priori knowledge for airborne TEM data inversion — A case study

Thomas Burschil [a,*], Helga Wiederhold [a], Esben Auken [b]

[a] Leibniz Institute for Applied Geophysics (LIAG), Stilleweg 2, 30655 Hannover, Germany
[b] Hydrogeophysics Group, Aarhus University, Høegh-Guldbergs Gade 2, DK-8000 Aarhus C, Denmark

ARTICLE INFO

Article history:
Received 11 October 2011
Accepted 1 February 2012
Available online 22 February 2012

Keywords:
SkyTEM inversion
Seismic reflection
A-priori information
Combined interpretation
North Sea island Föhr

ABSTRACT

We present a case study where a-priori knowledge from high resolution reflection seismic data is used to improve airborne time-domain electromagnetic data inversion. The a-priori knowledge constrains layer boundaries and lateral resistivity change during the inversion process.

The object for the case study is the North Sea island Föhr that was affected by several glaciations and inherits a complex Quaternary and Tertiary geology. The freshwater lens and the local geology were investigated by several geophysical surveys. A SkyTEM survey with following laterally constrained inversion provides the resistivity distribution of the island and several 2-D high resolution seismic reflection surveys give structural information. Vertical seismic profiles provide reliable velocity information for time-to-depth-conversion. Seismic horizons and a combined interpretation yield to a-priori constraints for the SkyTEM inversion.

We demonstrate how a-priori constraints enhance the inversion to a reliable direction. From the 3-D data cube of 1-D inversion models we extract an example and reinterpret the geophysical results. With the new inversion it is possible to image a till layer with subjacent sand in a larger range than before.

1. Introduction

Airborne electromagnetic surveys become more and more popular as the electric conductivity shows good correlation with structures relevant for groundwater research (e.g., Paine and Minty, 2005; Siemon et al., 2009). With airborne electromagnetics (AEM) a fast overview mapping of porous sedimentary layers like freshwater saturated sands, clay or till or saltwater intrusions is possible. Especially with time-domain transient electromagnetic soundings (TEM) an adequate depth penetration down to 200 m and more depending on the subsurface conductivity is feasible (Christiansen et al., 2009; Steuer et al., 2007). Huge datasets are gathered in a short time by contractors and after a careful editing or processing of the raw data a semi-automatic inversion is done to gain resistivity-depth models (e.g., Auken et al., 2009). By concatenating these 1-D models resistivity depth sections and maps are produced. Different types of inversion algorithms and inversion software are available (Zhdanov, 2010) and used, e.g., with few-layer models or smooth many-layer models. A defined number of layers are generally chosen for the models in the entire area, even if there are less or more geological layers. Lateral constraints along the flight lines or spatial constraints with neighboring data points in all direction assure flat models with small lateral variation (Auken and Christiansen, 2004; Christensen et al., 2009; Viezzoli et al., 2008). The resulting resistivity depth sections and maps often allow a direct delineation of hydrological or geological regions via resistivity contrasts. But what is the reliability or worth of these data or where are traps and what could be a practicable way to strengthen the interpretation? Several authors show that for the interpretation a combination of different geophysical methods provides best results (e.g., BURVAL Working Group, 2009). Large scale AEM in connection with 2-D high resolution seismic reflection and borehole data and logs yields spatial information of lithology and hydrogeological parameters (e.g., Gabriel et al., 2003; Høyer et al., 2011; Jørgensen and Sandersen, 2009; Jørgensen et al., 2003). All methods are generally measured and evaluated separately and the data are only combined in the interpretation. No or only a little information transfer during processing or inversion steps happened.

In this case study we insert information from high resolution seismic reflections in the inversion process of TEM data gained with the helicopterborne TEM system SkyTEM (originally described by Sørensen and Auken, 2004). Picked and interpreted horizons from several seismic lines give a-priori information to layer boundaries. This a-priori information leads the inversion to more reliable resistivity-depth models of the subsurface. A classification of geological units becomes more defined especially in a region of freshwater saturated sand, till and clay layers.

The German North Sea island of Föhr is part of a pilot area of the EU Interreg IVB project CLIWAT, whose main subject is to investigate the influence of climate change to groundwater systems in coastal areas. The island was surveyed with the SkyTEM system in 2008 (Wiederhold et al., 2010), high resolution seismic reflection in 2009 and 2010 and other geophysical methods (Fig. 1). Logs and geological

* Corresponding author. Tel.: +49 511 6433026.
E-mail address: Thomas.burschil@liag-hannover.de (T. Burschil).

0926-9851/$ – see front matter © 2012 Elsevier B.V. All rights reserved.
doi:10.1016/j.jappgeo.2012.02.003

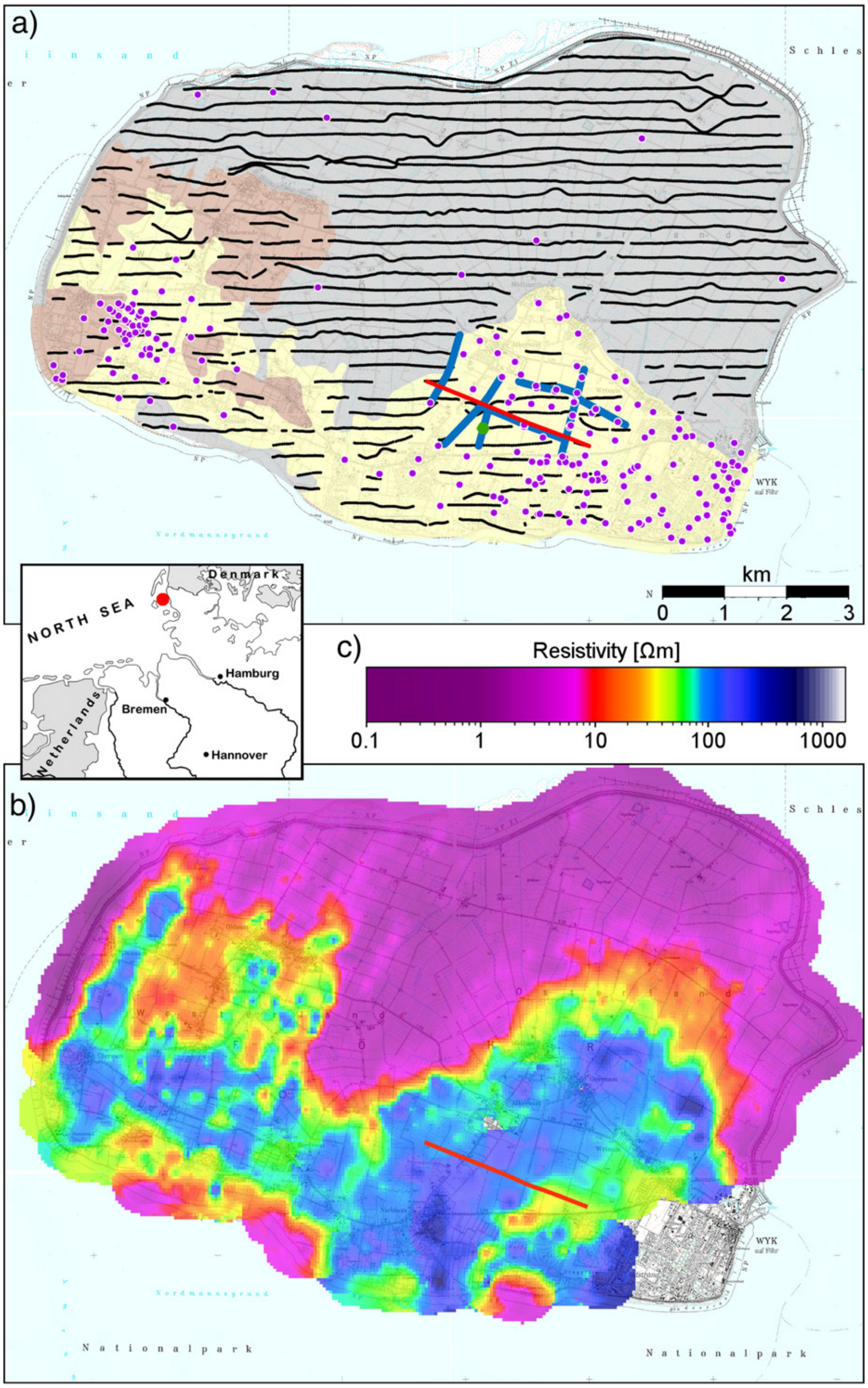

Fig. 1. Site plan of the North Sea island Föhr (DTK25© LVermGeo SH); a) Geological map (GÜK200© BGR1993) showing moraine area, e.g. sand/gravel (yellow), sand to silt (brown) and marshland, e.g. clay and silt (gray), and geophysical surveys, e.g. SkyTEM flight lines (black), seismic profiles (blue) and VSP in borehole Beo26 (green), and boreholes (purple). The red line marks the cross-section shown in Figs. 2, 4 and 5; b) average resistivity map for the range −20 m to −30 m MSL. The blue colors point to freshwater saturated areas or till; purple color points to saltwater-bearing sediments or clay; c) resistivity color scale used in this paper.

cross-sections from a dense borehole grid of the local waterworks describe the geological situation down to 130 m depth.

2. Geological situation

Föhr is a glacially overprinted island with moraine sediments (Geest) from Saalian age outcropping in the south and overlain by marshlands in the north (Fig. 1a). The island with about 10 km diameter is situated 7 km west off the North Sea Coast of Schleswig-Holstein, Germany's northernmost federal state. The area is affected by two glaciations (Elsterian and Saalian); the third north European glaciation (Weichselian) did not reach the western coast of Schleswig-Holstein (Ehlers and Gibbard, 2008). The water supply wells are restricted to the Geest area with elevations up to 13 m MSL where groundwater recharge takes place and a freshwater lens is developed (Steinmann and Ketelsen, 2004). This is not the case in the low-lying marshlands where saltwater intrudes (Fig. 1b). Important aquifer structures for the water supply are Quaternary meltwater sands and Tertiary sands. Quaternary sand and till layers have an average depth about 50 m, but can reach more than 120 m within buried glacial valleys. In the upper part sediments consist of alternating layers of Saalian fluvial sand and till, in some parts even Weichselian fluvial sand appears. The first till layer covers in a wide range a package of Saalian sand, which is most important for groundwater extraction. Two buried valleys were found by boreholes in the eastern Geest area and assumed to be carved during the Saalian glaciation. The western valley is smoothly dipping and filled with sand and till layers. The eastern buried valley is steeply dipping and filled mostly with till. Both valleys have small units of glacial fluvial sand at the bottom.

In the deeper part boreholes detected Pliocene kaolin sand and Miocene fine sand as well as mica clay. These Tertiary sediments form a glaciotectonic thrust-fault complex, recognized by abreast geological units. Maximal drilling depth of 130 m delimitates our geological information of this complex. The complex was formed during the Elsterian glaciation. A general description of glaciotectonic thrust-fault deformation is given by Aber and Ber (2007). The Pliocene and Miocene sand located west of the eastern buried valley is also a significant aquifer and used for nearly one-third of the local water extraction.

3. Geophysical data

3.1. Seismic data

Shallow high-resolution seismic reflection data provide good structural images of the subsurface. On Föhr we measured about 8 kilometers with the P-wave seismic method shared along seven profiles to get a better structural image and to improve the groundwater model. The hydraulically controlled vibrator system of LIAG (Buness and Wiederhold, 1999) was used as seismic source as well as planted z-component geophones as receivers. Acquisition parameters (Table 1) of receiver and source yield a common midpoint spacing of 1 m. Processing and evaluation was done with commercial processing software (Landmark ProMAX 2D Version 2003.12.1). Among conventional processing steps (e.g., Yilmaz, 2001) were tools like spectral whitening, dip move-out and normal move-out correction as well as common midpoint stacking.

Velocity analysis was done in an iterative way together with dip move-out correction to adjust velocities to dipping reflectors. For time-to-depth conversion we used interval velocities from a vertical seismic profile (VSP) located on one profile (Fig. 1a). Beneath 100 m depth the values were extrapolated by interval velocities calculated from stacking velocities. At the location of the borehole Beo26, where we measured the VSP, time-to-depth conversion works fine and we could identify layer boundaries by reflections. It is difficult to specify an error in depth estimation, because stacking velocities are arguable.

Final processing steps were finite-difference time migration and time-to-depth conversion with the aforementioned interval velocities (Fig. 2a,b).

Table 1
Seismic acquisition parameters of the Föhr survey.

Source (spacing)	LIAG MHV 2,7 & HVP-30 (4 m)
Sweep	30–240 Hz, 10 s, 2 vertical stacks
Receiver (spacing)	z-Geophone Sensor SM7 20 Hz (2 m)
Seismograph	Geometrics Geode, max. 264 channels
Recording, sampling, recording length	Correlated, 0.5 ms, 2 s

3.2. SkyTEM data

Airborne electromagnetic methods provide effectively large scale datasets of resistivity distribution. TEM systems are sensitive to low resistivity values (Christiansen et al., 2009), e.g., saltwater or clay. The survey of Föhr was part of a large-area airborne TEM campaign in northern Germany (Wiederhold et al., 2010). Data acquisition was done by SkyTEM ApS using the helicopterborne SkyTEM system (Sørensen and Auken, 2004) within two days. Target was the mapping of aquifers and aquitards as well as saltwater intrusions. To ensure good near surface resolution and good depth penetration a low and a high transmitter moment were used (Table 2). Aarhus Geophysics did the data processing and inversion within the Aarhus Workbench processing system. The recorded data show in general a good quality with not many distortions by man-made conductors.

The inversion was done with 1-D Lateral Constraint Inversion (LCI) using a 5 layer model as well as a smooth inversion with 19 layers (Christensen et al., 2009) for both transmitter moments together (Fig. 2c). No additional information on geology was included in the processing flow. A data example is given in Fig. 3. The 5 layer model, chosen for the entire island, is well fitting the data, but even a simpler, e.g. 3 layer model, would create an appropriate and comparable result. The resolution is decreasing by depth due to a wider footprint of the EM field (Auken et al., 2008, Høyer et al., 2011). In the case of LCI the 30 m thick till layer in the western buried valley is not resolved in a depth of 80 m.

The data were compared with ground-based TEM measurements and the results show similar resistivity distribution like airborne data (Liss et al., 2011, Steuer et al., 2011).

3.3. Interpretation of geophysical data — initial status

The seismic sections (example: Fig. 2a,b) resolve several sediment units in the subsurface that can be identified by the lithology columns of boreholes. Below −147 m MSL the reflection pattern is parallel and undisturbed and we interpret this boundary as a detachment of the thrust-fault complex. Above −147 m MSL the seismic sections show a complex image of the thrust-fault structure as well as refilled buried glacial valleys. By borehole logs and the reflection pattern we identify a large till layer in the western buried valley with a maximal thickness of 33 m (Fig. 2a).

For better comparison with the seismic results we define a special cross-section from the SkyTEM data volume. The resistivity cross-section of the 5 layer LCI (Fig. 2c) shows different features in the resistivity distribution. The 5th layer has a low resistivity value (<15 Ωm) and only a small lateral change. Maximal elevation of top 5th layer is around −180 m MSL at profile location 750 m. Above that a region with high resistivity (>80 Ωm) covers a lower resistivity range. Between 1000 and 1300 m these resistivity values of the 4th layer are in the range of 40–70 Ωm, where an ambiguous interpretation is possible (BURVAL Working Group, 2009). From profile location 1300 m on resistivity values between 10 and 30 Ωm point to Tertiary mica clay, as we know from the geological model. In the upper part of the cross-section resistivity values above >80 Ωm mark the freshwater saturated sand in the buried valley. Between profile location 1800 and 2400 m higher resistivity values point to kaolin sand and Miocene fine sand. Note, that last data points are at distance 2050 m, so that extrapolation to distance 2400 m is not reliable. A till layer with resistivity around 40 Ωm covers this sand unit, but is not resolved in the western part (1600–1800 m). A reliable interpretation from resistivity and seismic data (Fig. 2d) can only be done for a few parts of that cross-section (Fig. 2e). In the region with seismic we can characterize Quaternary sand and till as well as parts of mica clay and kaolin sand. Large ranges in the western and eastern part of the profile are difficult to interpret. Sparse SkyTEM data density in the eastern part is a consequence of a bad signal to noise ratio in that area.

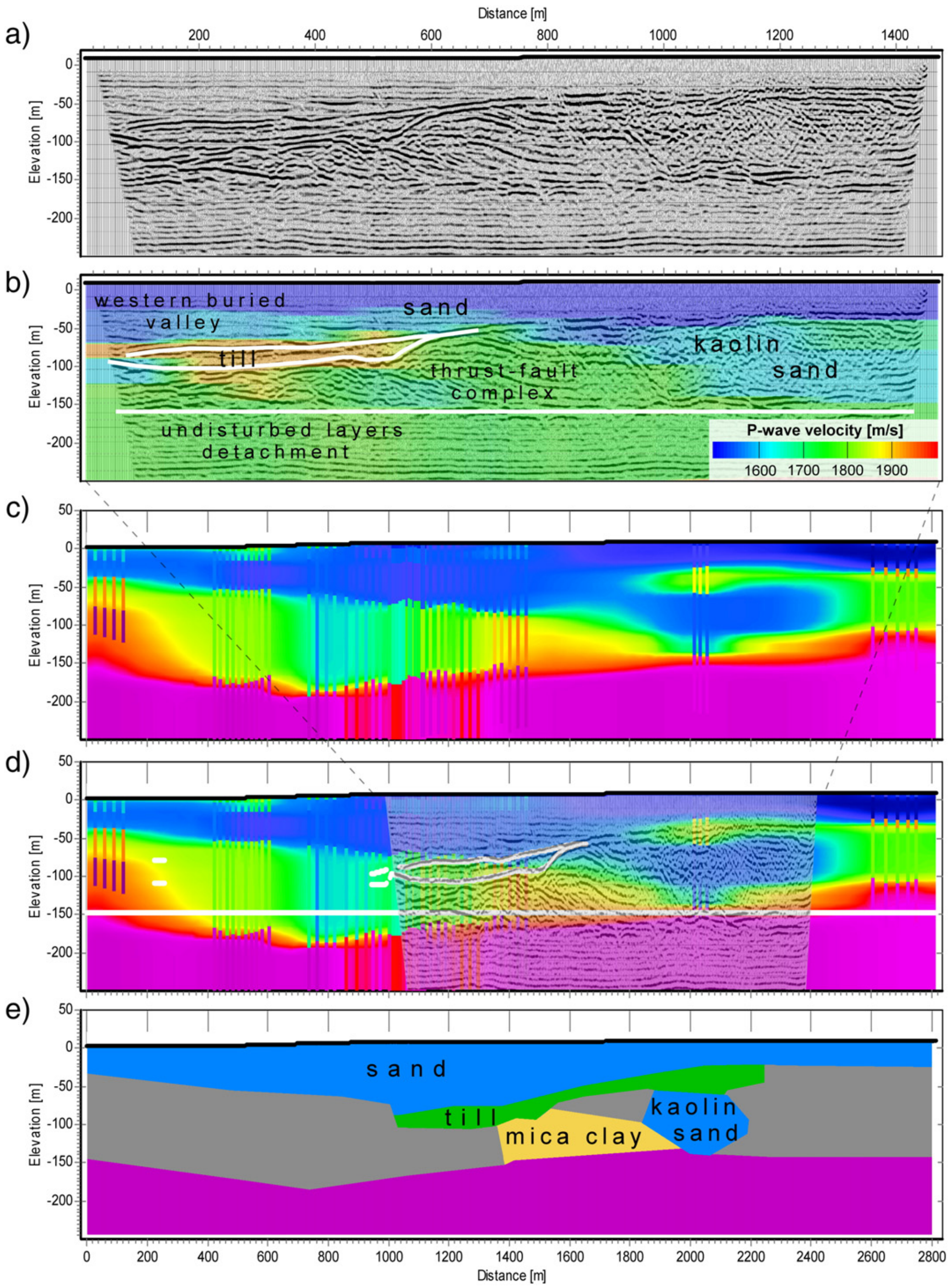

Fig. 2. Geophysical data, models and interpretation: a) seismic depth section (datum level 10 m MSL); b) seismic depth section with interval velocities and interpretation; c) vertical resistivity section from SkyTEM measurements (LCI, 5 layers). The columns show 1-D inversion results within 100 m radius to the cross-section, background color from 3-D grid; d) combination of a) and c) with seismic boundaries: detachment surface at −147 m, upper and lower boundary of till layer marked in seismic section and at two crossing seismic sections (compare Fig. 1a) by white lines; e) resulting geological interpretation, gray areas were not interpreted. Please note the differences in horizontal scales. For resistivity color scale see Fig. 1c.

Table 2
SkyTEM acquisition parameters of the Föhr survey.

Survey	306 profile km, 4 flights, 32 lines
Nominal ground speed	70–80 km/h
Line spacing, point spacing, depth of investigation	250 m, 20–30 m, 30–300 m
Time range, transmitter moment	10 µs–7 ms, 20750 Am² respectively 188000 Am²

4. Airborne TEM data inversion with a-priori knowledge

For AEM datasets 2-D or 3-D inversions, e.g. Ellis, 1998, Cox et al., 2010, are recently available, but for non-complex geology with adequate lateral change 1-D inversion with lateral or spatial constraints deliver appropriate quasi 3-D underground models (Christensen et al., 2009, Viezzoli et al., 2008). Constraints include boundary conditions and delimit changes of values within a defined deviation. Possible constraints for few-layer models are depth of layer boundaries, resistivity values or horizontal resistivity change.

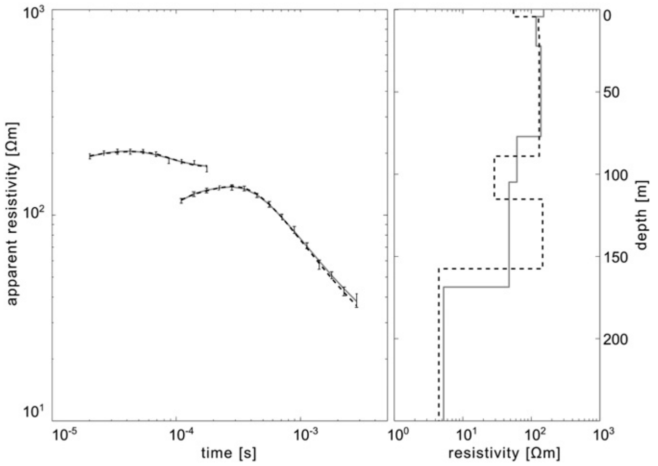

Fig. 3. Left: TEM data example with forward response for the low and high transmitter moment (black error bars) and two different inversion models: I (solid gray line) and V (dashed black line). Right: Depth model of inversion I (solid gray line) and V (dashed black line). The location of this example corresponds to distance 1135 m in Fig. 2c–e.

However, a-priori information can also be included into the inversion process. Such information can either be given as 1-D point information, e.g. from conductivity logs for resistivity values, or as 2-D information, e.g. from seismic horizons or other layer information. The a-priori values are imposed with deviation values and projected to surrounding data points.

The results from Section 3.3 suggest itself to use layer boundaries, i.e. picked seismic horizons, from the 2-D seismic depth section as a-priori information for the depth of layers as well as to limit the resistivity values for special regions, e.g., for the basement and the till layer.

In preparation for using a-priori information for the inversion and based on the knowledge of the local geology we first (I) reinverted the data with a 6-layer model and using Spatially Constrained Inversion (SCI, Viezzoli et al., 2008). The SCI takes neighboring data points in all directions into account and provides information transfer between the flight lines. Thereby a-priori constraints, e.g. from seismic lines, affect more TEM soundings in an indirect way than a LCI would do. Due to limited computational power the approximate forward response was used for the inversion process (Christensen et al., 2009).

Then, building on the initial interpretation (Section 3.3) we implemented a-priori information as constraints to the soundings step by step in the following way: (II) The undisturbed stratigraphy below −147 m MSL, which is found in all seven seismic sections, implies lateral resistivity constraints for the 6th layer and (III) an elevation boundary for the top of the 6th layer (−147 m MSL). Allowed changes for resistivity value and elevation are listed in Table 3. (IV) The picked horizons identified with the till layer constrain top and bottom of the 4th layer. The horizon depth values were projected onto soundings within a radius of 100 m. (V) In a last step we characterized the western buried valley via the previous inversion results and set the resistivity value of the till within the buried valley to a value of 28 Ωm.

Table 3
Constraints for different SkyTEM inversions (6 layer SCI). For results see Fig. 4; data and total residual are valid for the example shown in Fig. 3.

SCI	I	II	III	IV	V	Changes allowed
Strong laterally constrained resistivity of 6th layer		X	X	X	X	±0.5%
Top 6th layer constrained			X	X	X	−147 m MSL±1 %
Till layer (top/bottom of 4th layer) constrained				X	X	±10%
Resistivity of 4th layer constrained					X	28 Ωm ± 30 %
Data residual	0.451	0.446	0.552	0.605	0.594	
Total residual	0.289	0.359	0.384	0.385	0.390	

5. Results

Results of spatially constrained inversion with a-priori information are shown for the cross-section in Fig. 4 (II–V). Fig. 4 (I) shows the 6 layer SCI section as starting position. With avoiding lateral variation of the resistivity within the 6th layer (Fig. 4 (II)) this layer becomes more homogeneous as expected from seismic results. No significant changes were found in other parts of the cross-section.

With the second constrain (Fig. 4 (III)) the top of 6th layer is raised to −147 m MSL in the western part and the resistivity of the 5th layer increased between profile location 800 and 1200 m in comparison with the previous inversion results (Fig. 4 (II)). The boundaries of the 4th layer rise similarly.

Results of the third inversion step (Fig. 4 (IV)) differ from previous results. For the constrained 4th layer seismic horizons limit top and bottom boundaries and resistivity decreases to a value around ~30 Ωm. This value matches an expected value for till (Kirsch, 2009). Consequently the resistivity of the 5th layer increases to an interpretable value above >80 Ωm.

With the fourth inversion the value of the till layer was set to 28 Ωm with a deviation of 30% within the western buried valley. This behavior is warrantable because we identify the till layer in different location within this valley via borehole logs, reflection pattern from seismic data and previous inversion results. This constraint focuses the 4th layer and displays the till layer more explicitly (Fig. 4 (V)).

In Table 3 data and total residuals are shown for the inversions with different a-priori constraints. For SCI the entire area is divided into feasible parts and the inversion is run parallel (Viezzoli et al., 2008). The total residual is the residual of such a part and data residual is for each data point (Christensen et al., 2009). For different inversions the residual do not change significantly, so that a generally good data fit is done.

Within a new interpretation (Fig. 5) made from new resistivity models together with seismic large un-interpretable regions become more clear. A continuous 4th layer yields to a wide aquitard and the 5th layer with resistivity values above 80 Ωm suggests a wide freshwater saturated sand unit.

6. Discussion

A-priori information sets a framework for layer boundaries in inversions. But boundary conditions can also force the inversion to a not fitting result. Considering total residuals of different inversion results no large differences can be found (Table 3). Indeed, residuals increase a bit, but inversion still fits the data, as shown in the example in Fig. 4. A comparison of all five inversion results shows the splitting of the 4th and 5th layer as soon as we include the till layer boundaries (Fig. 3).

Within the results with the different a-priori information most data curves from the forward responses do not change a lot. We can find all features already more or less in the SCI without a-priori information (Fig. 4(I)). But each inclusion of a-priori information divides layers to a more structural result. The resistivity range of 50–80 Ωm is split in two interpretable parts and we can distinguish freshwater saturated sand, till and clay layers (Fig. 4 (V)).

Another possible source of error is the processing and time-to-depth conversion of the seismic data. Small changes in stacking velocities constitute large change in interval velocities. But time-to-depth conversion for all profiles was done with a single interval velocity function made of VSP velocities above 100 m depth and stacking velocities below 100 m depth. Seismic depth sections match several borehole logs on the profiles, so that no large error from time-to-depth conversion is expected.

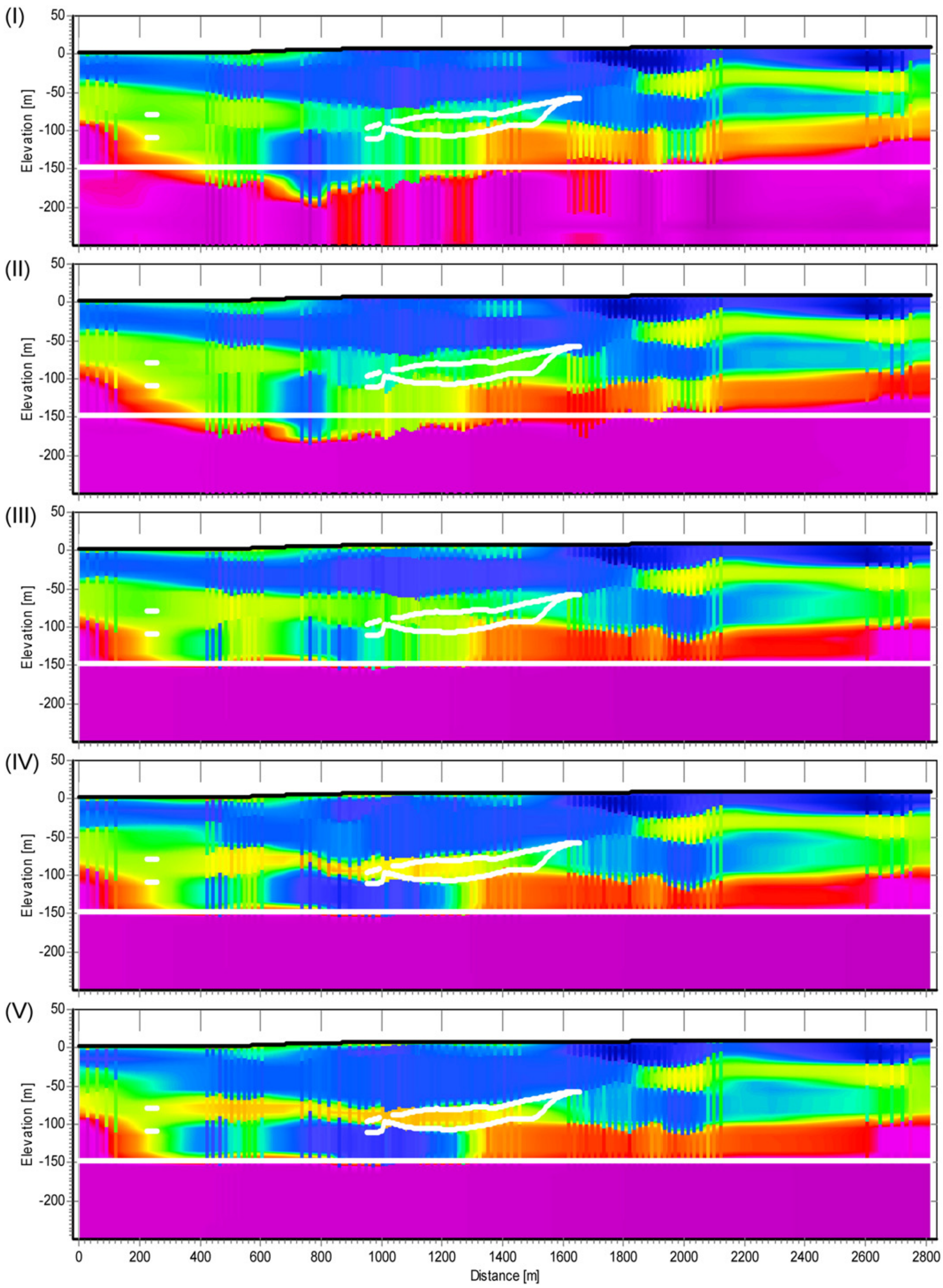

Fig. 4. Result of SCI with different constraints from a-priori information (white lines analogue Fig. 2d); (I) 6 layer SCI, (II) plus resistivity of 6th layer laterally constrained, (III) plus top 6th layer at −147 m MSL constrained, (IV) plus top and bottom of 4th layer from horizon picks constrained, (V) plus resistivity value of 4th layer constrained to 28 Ωm. The columns show 1-D inversion results within 100 m radius to the cross-section, background color from 3-D grid. For color scale see Fig. 1c.

The geology down to −147 m MSL depth is formed within two glacial periods and thus very inhomogeneous. On a small scale range we can find large spatial changes in different layers. Structures like the thrust-fault units (see Fig. 2) have lateral dimensions in a range of more than 200 m, so we avoid effects of these changes with a projection radius of 100 m for the till layer.

Few layer models have in general problems with dipping interfaces of two geological units. With 1-D inversion the models have to separate the transition zone into 2 layers. Together with depth constraints from a-priori seismic information it is not possible to resolve such a transition zone in a natural way. An example of this behavior is obvious in Fig. 5 at distance 1300 m. Seismic horizons show another transition region from clay to sand as the resistivity values suggest. A many layer model with small scale layer thickness would enhance the model here.

7. Conclusion

We have presented a case history from the island of Föhr with re-inversion of airborne TEM data constrained by a-priori information from seismic reflection sections. The results show that the interpretability of inversion results is enhanced. A prior to that not interpretable resistivity distribution becomes now significant.

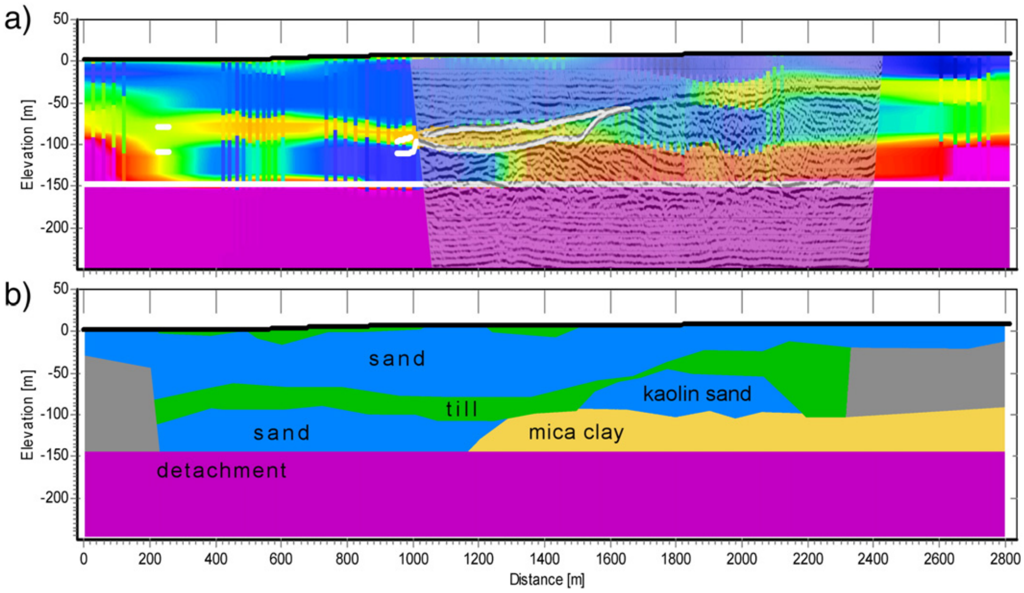

Fig. 5. a) Improved vertical section (seismic section and resistivity). For color scale see Fig. 1c, white lines analog Fig. 2d. b) Improved interpretation.

The seismic reflection sections itself deliver a good structural image of the underground but we cannot characterize units without additional and reliable information from boreholes, interval velocities or resistivity values. The resistivity values of the initial inversion of TEM data without a-priori information were not that reliable. But when extracted horizons from the seismic reflection interpretation were included in the inversion process the matching of resistivity distribution and seismic horizons is formidable. The combined interpretation creates a clear and reliable image of the subsurface and 3-D underground model. Geophysical investigation using reflection seismic method and airborne TEM crystallize as good tools in groundwater research.

Additional steps could be to include more horizons as a-priori information but more boundaries bear the risk of artificial effects. We also do not have a high data density in that region to get additional information. Another possible step is using a smooth 19-layer model for the inversion or a-priori information within full 3-D inversion. But such a tool is not available yet.

Acknowledgements

We thank Flemming Jørgensen, Wolfgang Scheer and Reinhard Kirsch for fruitful discussions about the local geology on Föhr. Further we thank the Landesamt für Landwirtschaft, Umwelt und ländliche Räume Schleswig-Holstein who made the unpublished reports about the Hydrogeology of Föhr available to us. I (TB) thank Aarhus University for hosting me and especially Bjarke Roth for a lot of help to deal with Aarhus Workbench.

This article is an outcome of the EU Interreg IVB project CLIWAT (ID 35-2-1-08). It has been co-funded by the North Sea Region Programme 2007-2013 under the ERDF of the European Union.

References

Aber, J.S., Ber, A., 2007. Glaciotectonism. Developments in Quaternary Sciences, 6. Elsevier, Amsterdam.
Auken, E., Christiansen, A.V., 2004. Layered and laterally constrained 2D inversion of resistivity data. Geophysics 69 (3), 752–761. doi:10.1190/1.1759461.
Auken, E., Christiansen, A.V., Jacobsen, L.H., Sørensen, K.I., 2008. A resolution study of buried valleys using laterally constrained inversion of TEM data. Journal of Applied Geophysics 65, 10–20. doi:10.1016/j.jappgeo.2008.03.003.
Auken, E., Christiansen, A.V., Westergaard, J.H., Kirkegaard, C., Foged, N., Viezzoli, A., 2009. An integrated processing scheme for high-resolution airborne electromagnetic surveys, the SkyTEM system. Exploration Geophysics 40, 184–192.
BURVAL Working Group, 2009. Buried Quaternary valleys — a geophysical approach. Zeitschrift der Deutschen Gesellschaft für Geowissenschaften 160 (3), 237–247.
Buness, H., Wiederhold, H., 1999. Experiences with a vibrator system for shallow high-resolution seismic. Extended Abstract. EAGE 61st Conference and Technical Exhibition, Helsinki.
Christensen, N.B., Reid, J.E., Halkjær, M., 2009. Fast, laterally smooth inversion of airborne time-domain electromagnetic data. Near Surface Geophysics 7, 599–612.
Christiansen, A.V., Auken, E., Sørensen, K., 2009. The transient electromagnetic method, In: Kirsch, R. (Ed.), Groundwater Geophysics — a Tool for Hydrogeology, 2nd Ed. Springer, Heidelberg, pp. 398–413.
Cox, L.H., Wilson, G.A., Zhdanov, M.S., 2010. 3D inversion of airborne electromagnetic data using a moving footprint. Exploration Geophysics 41 (4), 250–259.
Ehlers, J., Gibbard, P., 2008. Extent and chronology of Quaternary glaciation. Episodes 31, 211–218.
Ellis, R.G., 1998. Inversion of airborne electromagnetic data. Exploration Geophysics 29, 121–127.
Gabriel, G., Kirsch, R., Siemon, B., Wiederhold, H., 2003. Geophysical investigation of buried Pleistocene subglacial valleys in Northern Germany. Journal of Applied Geophysics 53, 159–180. doi:10.1016/j.jappgeo.2003.08.005.
Høyer, A.S., Lykke-Andersen, H., Jørgensen, F., Auken, A., 2011. Combined interpretation of SkyTEM and high-resolution seismic data. J. Phys. Chem. Earth 36 (16), 1386–1397. doi:10.1016/j.pce.2011.01.001.
Jørgensen, F., Sandersen, P.B.E., 2009. Buried valley mapping in Denmark: evaluating mapping method constraints and the importance of data density. Zeitschrift der Deutschen Gesellschaft für Geowissenschaften 160 (3), 211–223.
Jørgensen, F., Lykke-Andersen, H., Sandersen, P., Auken, E., Nørmark, E., 2003. Geophysical investigations of buried valleys in Denmark: an integrated application of transient electromagnetic soundings, reflection seismic surveys and exploratory drillings. Journal of Applied Geophysics 53, 215–228.
Kirsch, R., 2009. Petrophysical properties of permeable and low-permeable rocks, In: Kirsch, R. (Ed.), Groundwater Geophysics — a Tool for Hydrogeology, 2nd Ed. Springer, Heidelberg, pp. 1–22.
Liss, B., Steuer, A., Kirsch, R., Wiederhold, H., 2011. TEM-Messungen auf der Insel Föhr zur Erkundung der hydrogeologischen Gegebenheiten. Proceedings 71. Jahrestagung der Deutschen Geophysikalischen Gesellschaft (DGG), Köln Germany, EM P22.
Paine, J.G., Minty, B.R.S., 2005. Airborne hydrogeophysics. In: Rubin, Y., Hubbard, S.S. (Eds.), Hydrogeophysics. Springer, Dordrecht, pp. 333–357.
Siemon, B., Christiansen, A.V., Auken, E., 2009. A review of helicopter-borne electromagnetic methods for groundwater exploration. Near Surface Geophysics 7, 629–646.
Sørensen, K.I., Auken, E., 2004. SkyTEM — a new high-resolution helicopter transient electromagnetic system. Exploration Geophysics 35, 191–199.
Steinmann, F., Ketelsen, H., 2004. Problematik der Wasserbewirtschaftung der Insel Föhr. IHP/HWRP-Berichte, Heft 1, Koblenz, Germany.
Steuer, A., Siemon, B., Auken, E., 2007. A comparison of helicopter-borne electromagnetics in frequency- and time-domain at the Cuxhaven valley in Northern Germany. Journal of Applied Geophysics 67, 194–205. doi:10.1016/j.jappgeo.2007.07.001.
Steuer, A., Liss, B., Burschil, T., Wiederhold, H., Kirsch, R., 2011. Hydogeophysical investigations on the North Sea island Föhr using airborne and ground-based transient electromagnetics. Proceedings EGU General Assembly, Vienna Austria, Vol. 13. EGU2011-7997.

Viezzoli, A., Christiansen, A.V., Auken, E., Sørensen, K., 2008. Quasi-3D modeling of airborne TEM data by spatially constrained inversion. Geophysics 73 (3), F105–F113.
Wiederhold, H., Siemon, B., Steuer, A., Schaumann, G., Meyer, U., Binot, F., Kühne, K., 2010. Coastal aquifers and saltwater intrusions in focus of airborne electromagnetic surveys in Northern Germany. Proceedings 21. Salt Water Intrusion Meeting; Ponta Delgada/Azores, Portugal, pp. 94–97.
Yilmaz, Ö., 2001. Seismic Data Analysis: Processing, Inversion and Interpretation of Seismic Data. Soc. Explor. Geophys, Tulsa.
Zhdanov, M.S., 2010. Electromagnetic geophysics: notes from the past and the road ahead. Geophysics 75 (5). doi:10.1190/1.3483901 75A49-75A66.